arXiv:astro-ph/9810290v1 19 Oct 1998

Preprint LBNL-42330

First Order Kaon Condensate[†]

Norman K. Glendenning and Jürgen Schaffner-Bielich

Nuclear Science Division & Institute for Nuclear and Particle Astrophysics,
Lawrence Berkeley National Laboratory, MS: 70A-3307
Berkeley, California 94720

October 8, 1997

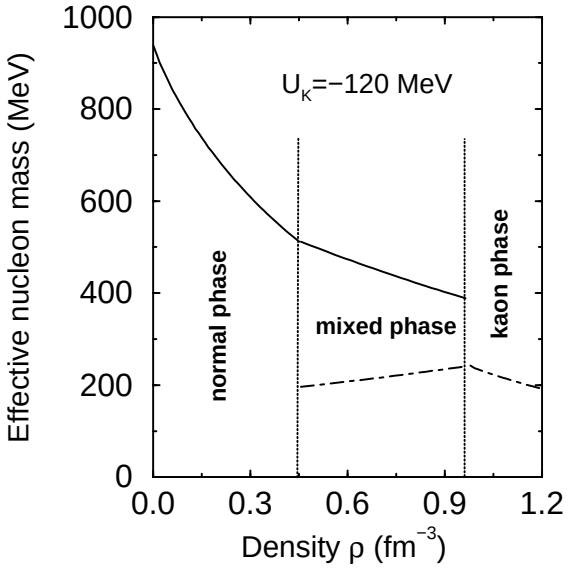

[†]This work was supported by the Director, Office of Energy Research, Office of High Energy and Nuclear Physics, Division of Nuclear Physics, of the U.S. Department of Energy under Contract DE-AC03-76SF00098.

[*][nkg/papers/kaon.tex, February 1, 2008

First Order Kaon Condensate

Norman K. Glendenning and Jürgen Schaffner-Bielich

Nuclear Science Division & Institute for Nuclear and Particle Astrophysics,
Lawrence Berkeley National Laboratory, MS: 70A-3307
Berkeley, California 94720

Abstract

First order Bose condensation in asymmetric nuclear matter and in neutron stars is studied, with particular reference to kaon condensation. We demonstrate explicitly why the Maxwell construction fails to assure equilibrium in multicomponent substances. Gibbs conditions and conservation laws require that for phase equilibrium, the charge density must have opposite sign in the two phases of isospin asymmetric nuclear matter. The mixed phase will therefore form a Coulomb lattice with the rare phase occupying lattice sites in the dominant phase. Moreover, the kaon condensed phase differs from the normal phase, not by the mere presence of kaons in the first, but also by a difference in the nucleon effective masses. The mixed phase region, which occupies a large radial extent amounting to some kilometers in our model neutron stars, is thus highly heterogeneous. It should be particularly interesting in connection with the pulsar glitch phenomenon as well as transport properties.

1 Introduction

Many phase transitions may occur in superdense matter. Among the possible new phases that have been considered over the past few years are pion and kaon condensed and quark deconfined matter. Transitions from the normal to any of these high-density phases may be of first or second order. The order depends in part on the strength of coupling constants. If of first order, especially interesting phenomena occur in isospin asymmetric nuclear matter, including spatially ordered regions of the normal and new phase in the range of densities for which both phases are in equilibrium [1, 2].

In early work on pion condensation, the region of phase coexistence was found by use of the Maxwell construction (sometimes with reference to Van der Waal's equation of state; cf. Refs. [3, 4, 5, 6, 7]). The Maxwell construction is valid for simple substances—those with *only one* independent component, like water, or pure neutron matter (which nowhere exists). However, as used[1], this construction can assure that only one chemical potential is common to the two phases, whereas asymmetric nuclear

[1]To be sure, the Maxwell construction could be generalized. But "equal areas" would be replaced by "equal volumes", and "tangent slope" by "tangent surface" in a space of $n+1$ dimensions, where n denotes the number of independent components.

matter, such as neutron star matter, has two independent components (the baryon and electric charge). Consequently the construction cannot satisfy Gibbs criteria that all chemical potentials as well as pressure and temperature be common to both phases in equilibrium. In short, the states studied were unstable.

Similarly the deconfinement transition was treated in early work beginning in the 1970's with the same assumptions and methods and without regard to equilibrium (in some cases without regard to beta equilibrium in the pure phases and in others without regard to phase equilibrium). The deconfinement phase transition for β stable matter has been treated recently in some detail taking account of equilibrium in all phases [1, 2, 8, 9, 10, 11, 12]. (The Gibbs criteria was used in Ref. [13, 14] in heavy-ion physics where it was essential for the distillation of strangeness.)

The possibility of kaon condensation was discussed already some years ago in the context of hyperonized neutron star matter [15]. But the real impetus for the recent interest was provoked by the paper of Kaplan and Nelson [16] who suggested the interaction of the K^- with the nuclear medium may reduce its mass sufficiently, so that, as a boson, it may replace electrons as the neutralizing agent in charge neutral matter. The Maxwell construction was again used in previous work on first order kaon condensation [17, 18, 19, 20].

In the present paper we study the kaon condensed phase as a *first order* phase transition in neutron star matter. This will serve as a general example of a Bose condensate (whether pion or kaon). Unlike the previously cited work, we assure compliance with Gibbs criteria for equilibrium. Just as in the case of the deconfinement phase transition, we find that the two phases in equilibrium are oppositely charged, though in sum, neutral, as ought to be so for stellar material. Consequently, the total energy, including Coulomb and surface energies, is minimized by a lattice arrangement of the rare phase immersed in the dominant [1, 2]. The difference between normal and kaon condensed phases is especially illustrated by the fact that not only are kaons present in the latter, but the nucleon masses are strongly modified from their values in the normal phase or in vacuum. Even in the spatial regions of the mixed phase occupied by the normal or condensed phase, the nucleons have different masses according to the phase [21]. The high degree of inhomogeniety in the mixed phase occupied as it is by a lattice structure, the localization of opposite charge in the phase occupying the lattice sites as compared with that of the background phase and the very different nucleon effective masses in the two phases, will likely affect the transport and superfluid properties of neutron stars.

The paper is organized as follows: in sec. 2 we introduce the model Lagrangian which is based on the relativistic mean-field model for the nucleon-nucleon interactions and a kaon-nucleon interaction motivated from one-boson exchange. We discuss the equation of state and especially the difference between a Maxwell construction and Gibbs condition as well as the properties of the mixed phase in Sec. 3. Consequences for the stellar properties are derived in sec. 4, both for global features as well as for the resulting geometrical structures inside neutron stars. Our results are summarized in sec. 5.

2 Relativistic Mean–Field Model with Kaons

In the approach presented here, we use a relativistic nuclear field theory solved in the mean-field approximation. The interaction between baryons is mediated by the exchange of scalar and vector mesons. This picture is consistently extended to include the kaons. The model is similar to the one used for describing the properties of the H dibaryon in nuclear matter which is known to be thermodynamically consistent [22]. The coupling schemes applied for the kaon are in analogy to the one we used for the H dibaryon [23].

We start by summarizing briefly the relativistic mean-field model for nucleons. The Lagrangian is given by

$$\begin{aligned}\mathcal{L}_N &= \bar{\Psi}_N \left(i\gamma_\mu \partial^\mu - m_N + g_{\sigma N}\sigma - g_{\omega N}\gamma_\mu V_\mu - g_{\rho N}\vec{\tau}_N \vec{R}_\mu \right) \Psi_N \\ &\quad + \frac{1}{2}\partial_\mu \sigma \partial^\mu \sigma - \frac{1}{2} m_\sigma^2 \sigma^2 - U(\sigma) \\ &\quad - \frac{1}{4} V_{\mu\nu} V^{\mu\nu} + \frac{1}{2} m_\omega^2 V_\mu V^\mu - \frac{1}{4} \vec{R}_{\mu\nu} \vec{R}^{\mu\nu} + \frac{1}{2} m_\rho^2 \vec{R}_\mu \vec{R}^\mu \quad , \end{aligned} \tag{1}$$

where $V_{\mu\nu} \equiv \partial_\mu V_\nu - \partial_\nu V_\mu$. The scalar meson is denoted by σ, the vector meson $\boldsymbol{\omega}$ by V_μ and the iso-vector $\boldsymbol{\rho}$ meson by R_μ. The scalar self-interactions $U(\sigma)$ are taken to be [24]

$$U(\sigma) = \frac{1}{3} b\, m_N (g_{\sigma N}\sigma)^3 + \frac{1}{4} c\, (g_{\sigma N}\sigma)^4 \quad . \tag{2}$$

The model parameters can be algebraically determined by five bulk properties of nuclear matter [25]. Here, for illustrative purposes, we choose one of the parameter sets used in [26] with the nuclear matter properties: $E/A = -16.3$ MeV, $\rho_0 = 0.153$ fm^{-3}, $a_{\rm sym} = 32.5$ MeV, $K = 240$ MeV, and $m^*/m = 0.78$. Other parameterizations will not change the overall feature of kaon condensation as discussed in this paper.

Now we discuss the inclusion of the kaon-nucleon interaction terms. There are two main schemes for including effects of kaon condensation in neutron star matter. One uses terms derived from chiral perturbation theory—the other couples the kaon to meson fields. We choose to take the latter approach so that nucleon and kaon interactions are treated on the same footing as pointed out above. The kaon is then coupled to the meson fields using minimal coupling

$$\mathcal{L}_K = \mathcal{D}_\mu^* K^* \mathcal{D}^\mu K - {m_K^*}^2 K^* K \tag{3}$$

where the vector fields are coupled via the standard form

$$\mathcal{D}_\mu = \partial_\mu + i g_{\omega K} V_\mu + i g_{\rho K} \vec{\tau}_K \vec{R}_\mu \quad . \tag{4}$$

Then the vector fields are coupled to a conserved current which is consistent with Ward identities. The form (4) results in another coupling term in the Lagrangian (3) of the form

$$2 g_{\omega K}^2 V_\mu V^\mu K^* K \tag{5}$$

in addition to the standard Yukawa coupling term which gives a nonlinear dependence of the kaon optical potential with density.

The scalar field is coupled to the kaon by analogy to the minimal coupling scheme of the vector fields

$$m_K^* = m_K - g_{\sigma K}\sigma \quad . \tag{6}$$

In addition to the standard linear Yukawa coupling term, it gives also a quadratic coupling term to the scalar field in the Lagrangian of the form

$$(g_{\sigma K}\sigma)^2 K^* K \quad . \tag{7}$$

This term is small compared to the linear Yukawa coupling term as it is suppressed by $g_{\sigma K}/(2m_K)$. Nevertheless, it will simplify the equations of motion considerably as we will show in the following.

The equation of motion for the kaon can be written as

$$\left[\mathcal{D}_\mu \mathcal{D}^\mu + {m_K^*}^2\right] K = 0 \quad . \tag{8}$$

The poles of the kaon propagator can then be determined by

$$-\omega_K^2 + m_K^2 + k^2 + \Pi_K(\omega_K, \vec{k}, \rho) = 0 \tag{9}$$

where the K^- self-energy in matter (the space components of the vector field vanish $V_i = \vec{R}_i = 0$) is given by

$$\begin{aligned} \Pi_K(\omega, \vec{k}, \rho) &= -2\omega_K \left(g_{\omega K} V_0 + g_{\rho K}\vec{\tau}_K \vec{R}_0\right) - \left(g_{\omega K} V_0 + g_{\rho K}\vec{\tau}_K \vec{R}_0\right)^2 \\ &\quad -2m_K g_{\sigma K}\sigma + (g_{\sigma K}\sigma)^2 \end{aligned} \tag{10}$$

and depends on the in-medium kaon energy ω_K. It is straightforward to derive the dispersion relation for s-wave condensation (i.e. for $\vec{k} = 0$) for the K^-

$$\omega_K = m_K - g_{\sigma K}\sigma - g_{\omega K} V_0 - g_{\rho K} R_{0,0} \tag{11}$$

which is linear in the meson fields. There appear additional source terms in the equation of motion for the meson fields if a kaon condensate is present

$$\begin{aligned} m_\sigma^2 \sigma &= -b\, m_N (g_{\sigma N}\sigma)^2 - c\,(g_{\sigma N}\sigma)^3 + g_{\sigma N}\rho_s + 2 g_{\sigma K} m_K^* K^* K \\ m_\omega^2 V_0 &= g_{\omega N}(\rho_p + \rho_n) - 2 g_{\omega K}(\omega_K + g_{\omega K} V_0 + g_{\rho K} R_{0,0}) K^* K \\ m_\rho^2 R_{0,0} &= g_{\rho N}\,(\rho_p - \rho_n) - 2 g_{\rho K}(\omega_K + g_{\omega K} V_0 + g_{\rho K} R_{0,0}) K^* K \quad . \end{aligned} \tag{12}$$

Note that the equation of motion for nucleons are unchanged. The conserved current associated with the kaons is derived by using

$$\begin{aligned} J_\mu^K &= i\left(K^* \frac{\partial \mathcal{L}}{\partial^\mu K^*} - \frac{\partial \mathcal{L}}{\partial^\mu K} K\right) \\ &= K^* i\partial_\mu K - (i\partial_\mu K^*) K - 2 g_{\omega K} V_\mu K^* K - 2 g_{\rho K}\vec{\tau}_K \vec{R}_\mu K^* K \quad . \end{aligned} \tag{13}$$

In the mean-field approximation, the K^- density is given by

$$\rho_K = -J_0^K = 2\left(\omega_K + g_{\omega K} V_0 + g_{\rho K} R_{0,0}\right) K^* K \quad . \tag{14}$$

For s-wave condensation we can use the dispersion relation (11) to get an expression for the scalar density of the kaon

$$2m_K^* K^* K = 2(\omega_K + g_{\omega K} V_0 + g_{\rho K} R_{0,0}) K^* K = \rho_K \tag{15}$$

which comes out to be the same as the vector density. This relation holds only for $\vec{k} = 0$ which is the case for cold neutron star matter and s-wave condensation. It is a result of our choice of the scalar coupling scheme (6). For the negatively charged kaon the equation of motion are then simplified to

$$\begin{aligned} m_\sigma^2 \sigma + b\, m_N (g_{\sigma N}\sigma)^2 + c\,(g_{\sigma N}\sigma)^3 &= g_{\sigma N}\rho_s + g_{\sigma K}\rho_K \\ m_\omega^2 V_0 &= g_{\omega N}(\rho_p + \rho_n) - g_{\omega K}\rho_K \\ m_\rho^2 R_{0,0} &= g_{\rho N}\,(\rho_p - \rho_n) - g_{\rho K}\rho_K \quad . \end{aligned} \tag{16}$$

The total energy density is given by

$$\epsilon = \epsilon_N + \epsilon_K \tag{17}$$

and has a contribution from the kaon condensate. The nucleon part consists of the standard terms (cf. Ref. [25])

$$\begin{aligned} \epsilon_N &= \frac{1}{2} m_\sigma^2 \sigma^2 + \frac{b}{3}\, m_N (g_{\sigma N}\sigma)^3 + \frac{c}{4}\,(g_{\sigma N}\sigma)^4 + \frac{1}{2} m_\omega^2 V_0^2 + \frac{1}{2} m_\rho^2 R_{0,0}^2 \\ &\quad + \sum_{i=N,l} \frac{\nu_i}{(2\pi^3)} \int_0^{k_F^i} d^3k \sqrt{k^2 + m_i^{*2}} \end{aligned} \tag{18}$$

The sum is over nucleons and leptons. In principle it could extend over baryons of the octet, but we neglect the higher members in the present study. The kaon contribution to the energy density reads

$$\epsilon_K = 2{m_K^*}^2 K^* K = m_K^* \rho_K \quad . \tag{19}$$

The kaon does not contribute directly to the pressure as it is a (s-wave) Bose condensate so that the total pressure

$$\begin{aligned} p &= -\frac{1}{2} m_\sigma^2 \sigma^2 - \frac{b}{3}\, m_N (g_{\sigma N}\sigma)^3 - \frac{c}{4}\,(g_{\sigma N}\sigma)^4 + \frac{1}{2} m_\omega^2 V_0^2 + \frac{1}{2} m_\rho^2 R_{0,0}^2 \\ &\quad + \sum_{i=N,l} \frac{\nu_i}{(2\pi^3)} \int_0^{k_F^i} d^3k \frac{k^2}{\sqrt{k^2 + m_i^{*2}}} \end{aligned} \tag{20}$$

is just the familiar expression known from relativistic mean field theory for nucleons and leptons only. Hence, the equation of state will be considerably softened if the kaon condensate is present. The pressure is modified only indirectly through the change of the meson fields by the additional kaon source terms which enter into the equations of motion (16). The total charge is then

$$q_N = \rho_p - \rho_e - \rho_\mu \tag{21}$$

$$q_K = \rho_p - \rho_e - \rho_\mu - \rho_K \tag{22}$$

in the normal and in the kaon condensed phase, respectively.

The above relations do not fix the amplitude of the kaon condensate K^*K. The charged kaon amplitude is zero unless the condition

$$\omega_K = \mu_{K^-} = \mu_e \tag{23}$$

can be fulfilled. Generally the electrochemical potential increases as the baryon density increases, since this will usually mean that the proton density increases. Moreover, the K^- effective mass in the medium decreases with increasing density. Therefore at some density the above threshold condition may be fulfilled. Since all kaons can condense in the lowest energy state, they become energetically more favorable than electrons as the neutralizing agent of positive charge. With further increase of density and decrease in kaon energy ω_K, the electrochemical potential will decrease and the electron population will decrease.

For the isospin partner of the K^-, the K^0, the condition for condensation to happen reads $\omega(K^0) = 0$. Hence, if there is no isovector potential for the kaons, the K^0 can only appear after charged kaons have appeared and the electrochemical potential hits zero. This seems quite unlikely and, to our knowledge, was therefore completely ignored in previous works. Nevertheless, the isospin potential of the nucleons shift the energy of the K^0 below the one of the K^- in neutron-rich matter so that

$$\omega(K^0) = \omega(K^-) + 2g_{\rho K}R_{0,0} = \omega(K^-) - 2\frac{g_{\rho K}^2}{m_\rho^2}\left(\rho_n - \rho_p\right) \quad . \tag{24}$$

A strong isovector potential is supported by coupled channel calculations for the K^- [27] which shifts the effective energy of the K^- up by approximately 100 MeV at a density of $\rho = 3\rho_0$. This would imply that the effective energy for the K^0 is about 200 MeV lower than the one for the K^- in neutron matter at that density! In our calculations, we find indeed that K^0 condensation can happen if the isovector coupling constant is chosen as strong as the nucleon one (see eq. (25) in the following). For the sake of simplicity we ignore it in the following but note that it is clear from our discussion that K^0 condensation should be taken into account in a more realistic calculation.

The Lagrangian for the kaons (3) describes the kaon-nucleon interaction as well as the kaon-kaon interaction. The K^- in a nuclear medium is certainly a coupled channel problem due to the opening of the $\Sigma\pi$, $\Lambda\pi$ channels and can not be treated on the mean-field level. Coupled channel calculations at finite density, first done by Koch [28], yield an attractive potential for the K^- at normal nuclear density of about $U_{K^-}(\rho_0) = -100$ MeV. Waas et al. find a value of $U_{K^-}(\rho_0) = -120$ MeV [29]. Kaonic data support the conclusion that there is a highly attractive kaon optical potential in dense nuclear matter [30]. Because the kaon is a boson it does not add directly to the pressure; it forms a Bose condensate in the s-wave with zero momentum [16]. This is contrary to pion condensation which condenses in a p-wave with a finite momentum. A selfconsistent treatment of the in-medium self energy of the pion prevents pion condensation [31]. A coupled channel calculation including the modified self-energy

of the kaon has been studied in [32] and it was found that the kaon still sees an attractive potential at high density.

On the mean-field level considered here, the three kaon coupling constants, $g_{\sigma K}$, $g_{\omega K}$, and $g_{\rho K}$ can be fixed to kaon-nucleon scattering lengths. The in-medium potentials for the K^- are given by G-parity, i.e. by switching the sign of the vector potential. This gives similar results for the K^- optical potential compared to the coupled channel calculations [33]. We choose to couple the vector fields according to the simple quark and isospin counting rule

$$g_{\omega K} = \frac{1}{3} g_{\omega N} \quad \text{and} \quad g_{\rho K} = g_{\rho N} \quad . \tag{25}$$

The scalar coupling constant is fixed to the optical potential of the K^- at ρ_0:

$$U_K(\rho_0) = -g_{\sigma K}\sigma(\rho_0) - g_{\omega K} V_0(\rho_0) \tag{26}$$

The kaon potential is fixed at normal nuclear density and varies as a function of the density ρ.

We solve the equations of motions in three different ways corresponding to the three possible solutions: 1) for pure nuclear matter without kaons, 2) for pure kaon condensed matter, 3) for the mixed phase. The latter one is found by solving for solution 1) and 2) separately and scanning through the electrochemical potential until the pressures in the two phases for the same chemical potentials are equal. Initially, values for the meson fields are taken randomly. The solution found at a certain baryochemical potential is then used for the next step. We compare then the pressure of the three solutions and take the one with the highest pressure. It turns out that this procedure ensures automatically that the solution for the mixed phase gives a (thermodynamically consistent) volume fraction between zero and one.

3 Equation of State with a Kaon Condensate

In the following we discuss the equation of state including kaons emphasizing the difference between the hitherto applied Maxwell construction and the thermodynamic consistent Gibbs condition. Then we present our results for the two phases in the mixed phase.

3.1 Maxwell versus Gibbs

The standard thermodynamic rule for two phases in thermodynamical equilibrium is given by the Gibbs condition

$$p^{\mathrm{I}} = p^{\mathrm{II}}\,, \quad \mu_i^{\mathrm{I}} = \mu_i^{\mathrm{II}}\,, \quad T^I = T^{II} \tag{27}$$

which simply states that the two phases are in mechanical, chemical and thermal equilibrium. This is basic thermodynamics and can be found in textbooks. For the special case of only *one* chemical potential, the resulting equation $p^{\mathrm{I}}(\mu, T) = p^{\mathrm{II}}(\mu, T)$

has a unique solution for μ. It is often found by use of a Maxwell construction in one form or another. For example, the common tangent method, is based on the fact that $\mu = d\epsilon/d\rho = dE/dN$. Write the equation of state in the form $\epsilon = \epsilon(\rho)$. The segment of the common tangent, $\epsilon = -p_0 + \mu_0\rho$ touching the equation of state once in each phase describes the mixed phase with common and constant values of p_0 and μ_0, independent of the proportion of the two phases. Clearly, the Maxwell construction can assure that only a single chemical potential is common to both phases.

However, neutron star matter has two chemical potentials, μ_B and μ_e, each of which must be equal in the two phases to assure equilibrium. Hence, a Maxwell construction *cannot* be used as it will produce a discontinuity in one of the chemical potentials and will describe an unstable state—one for which there is a potential difference at the boundary between phases. This general fact concerning phase transitions with more than one conserved charge inside neutron stars was realized only a few years ago [1, 2]. It was shown how to assure equilibrium in substances of an arbitrary number of conserved charges, that conservation laws cannot be locally imposed but only globally over the entire region of mixed phase, how internal forces redistribute conserved charges between equilibrium phases so as to minimize the energy, and how, in the case that the electric charge is among the conserved charges, a Coulomb lattice will be formed.

Conservation laws and Gibbs conditions can be satisfied simultaneously for substances of more than one conserved charge by applying the conservation law(s) only in a *global* rather than a *local* sense [1, 2]. Thus for neutron star matter which has two conserved charges, the Gibbs conditions and conservation of electric charge read

$$p_N(\mu_B, \mu_e) = p_K(\mu_B, \mu_e) \tag{28}$$

$$q_{\rm total} = (1-\chi)q_N(\mu_B, \mu_e) + \chi q_K(\mu_B, \mu_e) = 0\,. \tag{29}$$

where q denotes charge density of the corresponding phase. This pair of equations can be solved for μ_B, and μ_e for any volume proportion of kaon phase χ in the interval (0,1). Therefore the chemical potentials are functions of proportion χ and therefore also are all other properties of the two phases, including the common pressure. This is only a mathematical proof that in general, properties will vary as the proportion. *Why* and how they vary depends on how the internal driving forces can exploit the degrees of freedom (one less than the number of independent chemical potentials) so as to minimize the total energy [2].

The total baryon density in the mixed phase corresponding to the solution of the above pair of equations for charge neutral matter in phase equilibrium is given as a function of χ by

$$n_{\rm total} = (1-\chi)n_N(\mu_B, \mu_e) + \chi n_K(\mu_B, \mu_e)\,, \tag{30}$$

where n denotes baryon number density. A similar equation holds for the energy density. It will be noted that the pressure equality (28) cannot be solved simultaneously with conditions of *local* charge neutrality, $q_N(\mu_B, \mu_e) = 0$, $\quad q_K(\mu_B, \mu_e) = 0$, since three conditions must be satisfied with only two variables.

Figure 1 shows the behavior of the chemical potentials using Gibbs and Maxwell construction for comparison. The vertical dotted lines indicate the region of the mixed

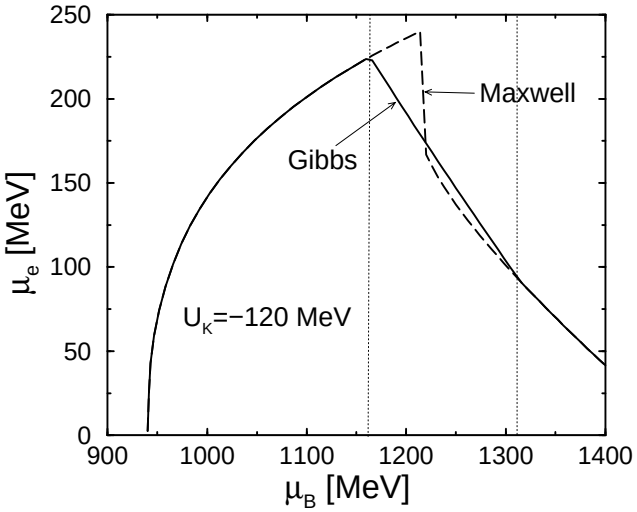

Figure 1: The two chemical potentials, the electrochemical potential and the baryochemical potential for the case $U_K(\rho_0) = -120$ MeV using the Gibbs condition (solid line) and a Maxwell construction (dashed line). The large electric potential difference that occurs for the Maxwell construction gives rise to an instability.

phase when using the Gibbs condition implemented for charge neutrality as described above. The electrochemical potential increases in the pure hadronic phase as the density of neutrons and protons increase. However, at the critical density for kaon condensation the electrochemical potential becomes a decreasing function of density as kaons replace electrons in their role of neutralizing the charge on protons. We note that when the conservation of electric charge is imposed as a global constraint, as described above and in Ref. [2], the electrochemical potential is continuous, in contrast to the case of the Maxwell construction. In the Maxwell construction, the electrochemical potential drops from $\mu_e = 240$ MeV to $\mu_e = 167$ MeV at the phase boundary resulting in a huge difference in the Fermi energy of the leptons between the two phases. There needs to be an additional force to prevent the electrons moving from the phase with the higher chemical potential to the other which is completely absent in a bulk treatment.

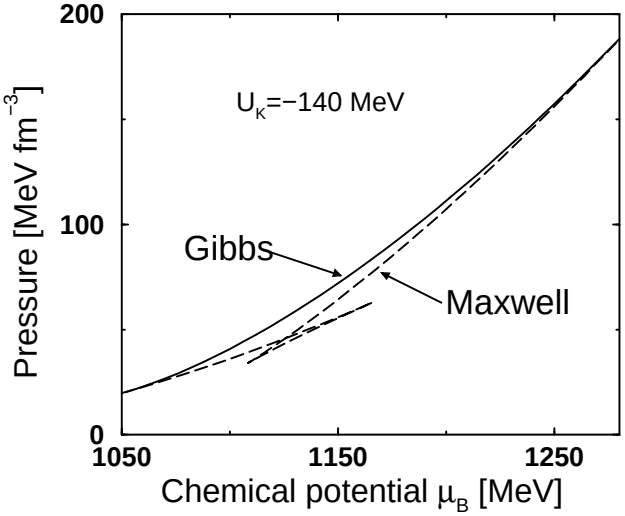

Figure 2: The pressure versus the baryochemical potential for a Maxwell construction (dashed line) compared to the Gibbs condition (solid line). The Gibbs condition is thermodynamically more stable.

A Maxwell construction is often implemented by looking at the thermodynamical potential of interest, here the pressure, as a function of the chemical potential as depicted in Fig. 2. The crossing of the curve is the point of equal pressure at the same baryochemical potential. Using the Gibbs conditions (27), the solid curve results which has always a higher pressure compared to the Maxwell construction being the thermodynamically favored one. The change in the slope at the crossover of the Maxwell construction is smeared out. The pressure difference between the two cases depends on the equation of state and the optical potential of the kaon. In addition, it is also sensitive to finite size corrections. Here, we discuss only bulk matter. Coulomb

energy and surface energy will reduce the pressure in the mixed phase. For the mixed phase of normal nuclear matter and nuclei in the crust of the neutron star, this correction is on the order of 10 MeV/fm[1]. It depends on the surface tension which is unknown for a kaon condensed phase immersed in dense nuclear matter and will shift the curve for the Gibbs condition case to slightly lower values. But because the sum of Coulomb energy and surface energy vanishes at the boundaries of the mixed phase (cf. eq. (2) in Ref. [10]), the boundaries are unaffected. We will discuss the geometric features when kaons are condensing in more detail later.

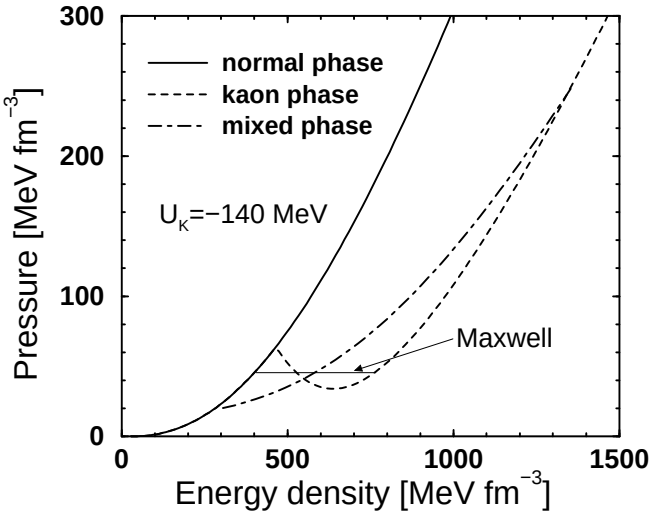

Figure 3: The equation of state for a pure nuclear matter (solid line), pure kaon matter (dotted line) for $U_K(\rho_0) = -140$ MeV. The Maxwell construction is shown by the horizontal line, the Gibbs solution by the dashed-dotted line.

The differences between the two descriptions, Maxwell and Gibbs, are most striking for the relevant observable for neutron star calculations: the equation of state as plotted in Fig. 3. The solid line shows the equation of state for the normal hadronic phase of neutron star matter, the dotted line the one for pure kaon condensed matter. The Maxwell construction results in a region of constant pressure (solid horizontal line) connecting the two different equation of states. Applying the Gibbs condition causes two major differences compared to the Maxwell construction. First, the region of constant pressure vanishes and there is a continuous increase of the pressure. Second, the density range of the mixed phase is much wider, it starts at a lower density and ends at a much higher density. Hence, the mixed phase can well be the dominant portion of a neutron star.

The behavior of the thermodynamic potential, the pressure, and the two chemical potentials over the mixed phase region using the Gibbs condition is summarized in Fig. 4. The baryochemical potential as well as the pressure are continuously rising

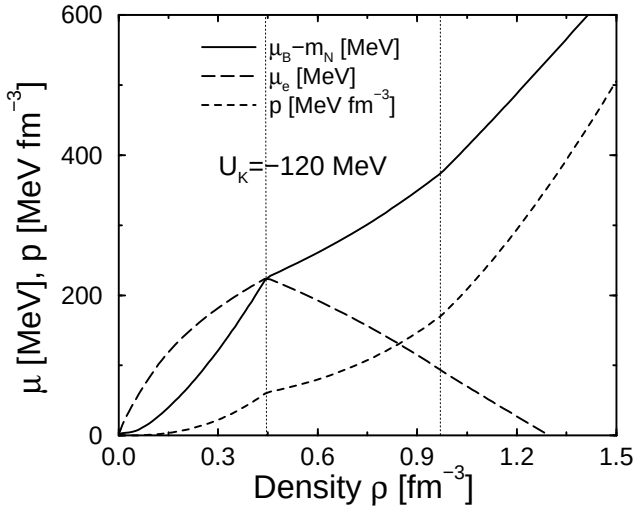

Figure 4: The pressure, the electrochemical potential, and the baryochemical potential are plotted over the mixed phase region using the Gibbs condition.

with density. The electrochemical potential increases until the mixed phase starts, then it is continuously decreasing with density. There is now no jump in any of these observables and none stays constant over the mixed phase region.

The form of the equation of state depends sensitively on the chosen optical potential of the kaon. Figure 5 shows the equations of state for optical potentials of the kaon at normal nuclear matter density between –80 and –140 MeV. For $U_K(\rho_0) = -80$ MeV, there is no mixed phase and the phase transition is of second order. For a deeper optical potential, a mixed phase appears as plotted in dashed-dotted lines. The deeper the optical potential of the kaon is, the lower is the density the mixed phase starts and the wider is the range of the mixed phase. The equation of state is considerably softened by the presence of the kaon condensate. The critical density for the onset of the kaon condensed phase is summarized for various kaon optical potentials in Table 3.1. For the cases $U_K(\rho_0) = -80$ MeV and -90 MeV the phase transition is of second order.

$U_K(\rho_0)$ (MeV)	–80	–90	–100	–110	–120	–130	–140	–150
ρ_c/ρ_0	4.5	4.2	3.8	3.4	2.9	2.4	1.8	1.2

Table 1: The critical density for the appearance of the kaon condensed phase for different kaon optical potentials.

Fig. 6 shows the populations of the nucleons, leptons and kaons for the case

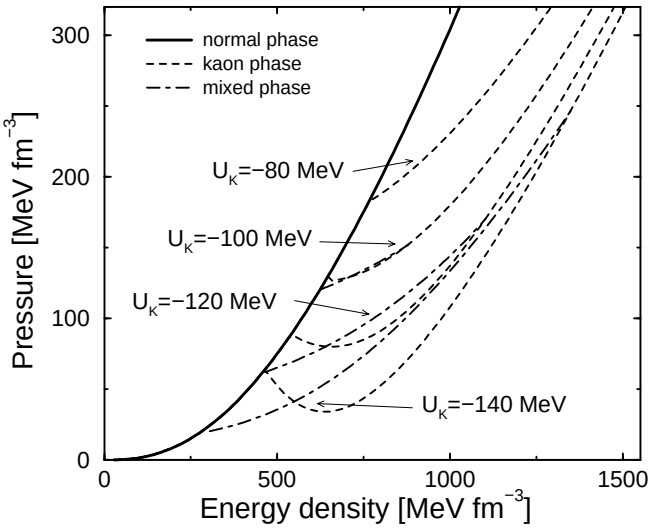

Figure 5: The equation of state for various choices of the optical potential of the kaon.

$U_K(\rho_0) = -120$ MeV. The remarkably feature is the 'frozen' neutron density once kaons start to condense. As it is more favorable to produce kaons in association with protons, the neutron density just stays (nearly) constant over the whole density range shown starting with the critical density. The lepton populations decrease as the K^- appears as the new neutralizing agent.

The neutron density seems to be frozen once kaons appear in the system as viewed on a logarithmical scale, but it actually varies slowly, going up and then down slightly with density at the order of a few percent. Note that the overall neutron density in the mixed phase is the sum of the two contributions from the normal and the kaon phase which makes it even more puzzling. The neutron population does even not change when the pure kaon phase is reached. Nevertheless, comparison with previous work on kaon condensation also indicates that the neutron population does not change very much once kaon condensation sets in. From Tables 3 and 4 in Ref. [34] one can read off the neutron density and finds that it changes at the level of a few percent up to moderate densities. This holds also for the calculations done by Fujii et al. [19]. The neutron density actually decreases first after kaons have appeared then it rises again for larger densities. The actual change in the neutron density is less than 10% up to a density of $\approx 5\rho_0$ after kaons have condensed [35].

Figure 7 shows the population in the mixed phase for the two phases separately as a function of volume proportion χ of condensed phase. The normal phase population is denoted as I, the kaon phase population as II. For $\chi = 0$ the proton population in the normal phase is small and neutrality is achieved by a balance with the sum of the lepton populations. This corresponds to local neutrality in the pure phase. However with a growing fraction of condensed phase, charge neutrality is achieved

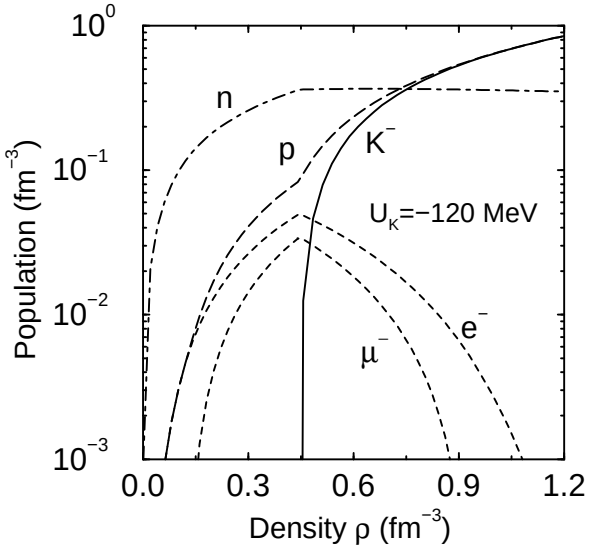

Figure 6: The population as a function of the nucleon density. The neutron density stays nearly constants once kaon condensation appears.

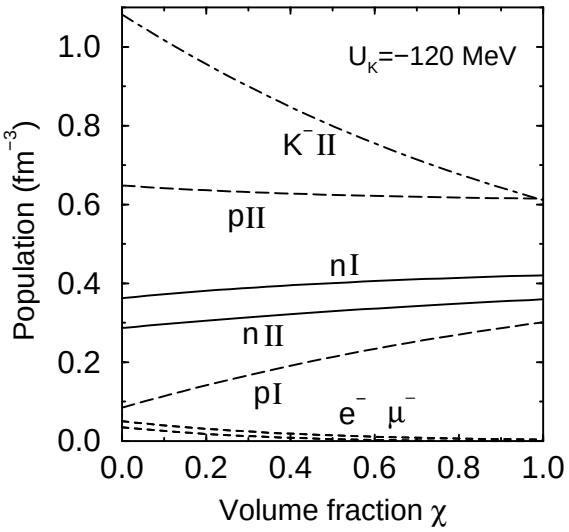

Figure 7: The population as a function of volume fraction of kaon condensed phase. Normal phase is denoted by I and condensed phase by II. Note the finite charge density in the condensed phase (negative) and normal phase (positive) which vanish only on the boundaries $\chi = 1$ or 0.

more economically between the two phases in equilibrium as a global constraint—the proton population increases to near equality with neutrons as the proportion of condensed phase increases, while the lepton populations decrease to the vanishing point. Isospin symmetry is thus closely achieved in the normal phase. This behavior is expected and explained in Ref. [2] as a general feature of the action of the isospin driving force toward symmetry in phase transitions of asymmetric nuclear matter.

The population behaviors in the condensed phase are different. We can understand this as follows: compare the energy of neutron and of a proton-K^- pair, whose chemical potentials are the same. They are respectively

$$\begin{aligned} \mu_n = E_n &= \sqrt{m^{\star 2} + k_{F,n}^2} + g_{\omega N} V_0 - g_{\rho N} R_{0,0} \qquad (31) \\ \mu_n = \omega_{K^-} + E_p &= m_K - g_{\sigma K}\sigma - \frac{1}{3} g_{\omega N} V_0 - g_{\rho N} R_{0,0} \\ &\quad + \sqrt{m^{\star 2} + k_{F,p}^2} + g_{\omega N} V_0 + g_{\rho N} R_{0,0} \\ &= m_K - g_{\sigma K}\sigma + \sqrt{m^{\star 2} + k_{F,p}^2} + \frac{2}{3} g_{\omega N} V_0 \,. \qquad (32) \end{aligned}$$

From these two expressions of μ_n we have,

$$\sqrt{m^{\star 2} + k_{F,p}^2} = \sqrt{m^{\star 2} + k_{F,n}^2} + \frac{1}{3} g_{\omega N} V_0 - g_{\rho N} R_{0,0} \,, \qquad (33)$$

from which it is clear that $k_{F,p} > k_{F,n}$ when the sum of the last two terms is positive. Since V_0 is proportional to the density, whereas R_{00} is proportional to the difference in isospin densities of proton and neutron, the sum will generally be positive, and is in the present case. That is, p-K^- pairs are preferred to neutrons. However, the symmetry restoring term in the energy will prevent an uninhibited growth of protons compared to neutrons.

We have neglected K^0 condensation (as has everyone else). It is clear that eventually there will be a competition between p-K^- pairs and n-K^0 pairs. It appears that with increasing density, the condensed phase will tend toward symmetry in neutrons and protons and similar density of K^- and K^0.

3.2 Mixed phase properties

We will show in the following that the two phases in equilibrium in the mixed phase have completely different properties. We will focus on the case $U_K = -120$ MeV in this section.

One striking question is, why should the nucleons not be the same in the two phases and why can they not move freely between phase I and phase II. The answer is that when the nucleons are treated as dynamical particles they are different in the two phases. Their interaction with the kaon field is what causes the decrease of the kaon effective mass with increasing density. The decrease in kaon mass ultimately leads to the condensation of kaons. The interaction also changes the nature of a nucleon. Figure 8 illustrates the dynamical nature of the nucleon: its effective mass is shown

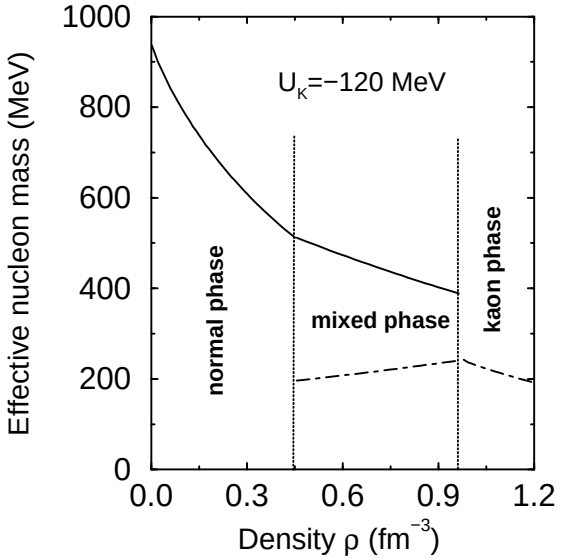

Figure 8: The effective nucleon mass as a function of the nucleon density. Shown by vertical lines is the onset and offset of the mixed phase.

as a function of baryon density. Up to $\rho = 0.45$ fm^{-3} there exists only one solution—the pure nucleon phase. The effective mass decreases with density from its vacuum value to 0.78 of its vacuum value at the saturation density of symmetric matter and further down to $m_N^* = 510$ MeV at the end of the pure normal phase ($\sim 3\rho_0$). In the mixed phase, a second solution appears at a much lower effective nucleon mass of $m_N^* = 196$ MeV. The second solution is the nucleon effective mass in the kaon condensed phase fraction of the mixed phase. The mixed phase ends at $\rho = 0.97$ fm^{-3} and only the second solution continues, now changing slope and decreasing with density. The nucleons have different effective masses due to the different mean-fields in the two phases in equilibrium. Hence, the nucleons cannot move freely between the two phases and a phase boundary can develop. In ref. [18] the nucleons in the two phases were treated only implicitly through a phenomenological equation of state. They did not appear as dynamical degrees of freedom, so the two solutions could not be found.

Figure 9 depicts the analogue to Fig. 8 for the effective energy of the kaon. Note that the kaon is only a test particle in the nucleon (normal) phase and appears only physically in the condensed phase. The effective kaon energy decreases with density due to the attractive vector interaction with nucleons, but kaons do not appear in the medium until the threshold condition discussed above is satisfied. However, we can trace the energy of a test kaon in the medium and it is shown in Fig. 9 as dashed-dotted line. Its energy as a test particle is also shown in the regions of the mixed phase that are occupied by the normal phase. When the kaon energy sinks to a value satisfying the threshold condition, kaons begin to appear, but because the

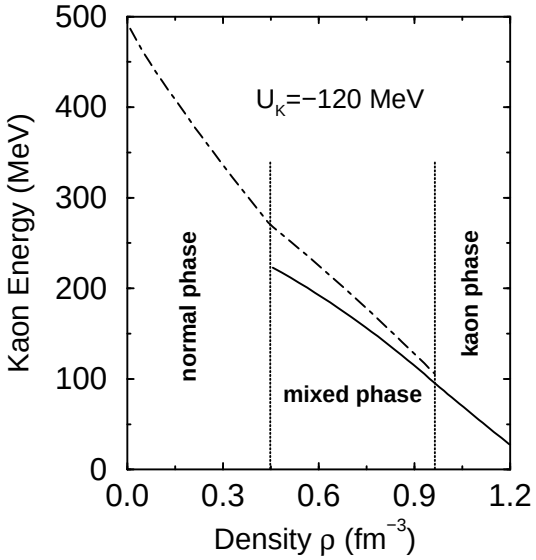

Figure 9: The effective kaon energy versus the nucleon density.

phase transition is first order they first appear in a small fraction of the total volume which is the kaon condensed phase in equilibrium with the normal phase. The energy of these medium modified kaons is less than that of a test kaon in the normal phase. The two energies are shown in the figure.

The most pronounced differences between the two phases is in the energy density and the charge density. As can be read from Fig. 10, the energy density of the nucleon phase (solid line) at the onset of the mixed phase is $\epsilon = 460$ MeV fm^{-3} while it amounts to $\epsilon = 1140$ MeV fm^{-3} for the kaon condensed phase (dashed line). The dashed-dotted line is the sum of the energy density of the two phase according to their volume fraction χ:

$$\epsilon = (1-\chi)\epsilon_N(\chi) + \chi\epsilon_K(\chi) \tag{34}$$

and is continuously growing with density but *not* linearly, as is the case in the Maxwell construction ($\epsilon_K(\chi)$ denotes the total energy density of the kaon phase and should be distinguished from eq. (19)). The non-constant pressure is of course associated with the non-linearity.

4 Stellar Properties

4.1 Large scale features

We have already stressed how differently the computed equation of state and matter properties are, depending on whether the Maxwell construction is used to determine (incorrectly) the mixed phase of normal and condensed phase, or whether Gibbs criteria for equilibrium are fully respected. We start our discussion of the large scale properties of stars by illustrating the difference in the mass-energy distribution

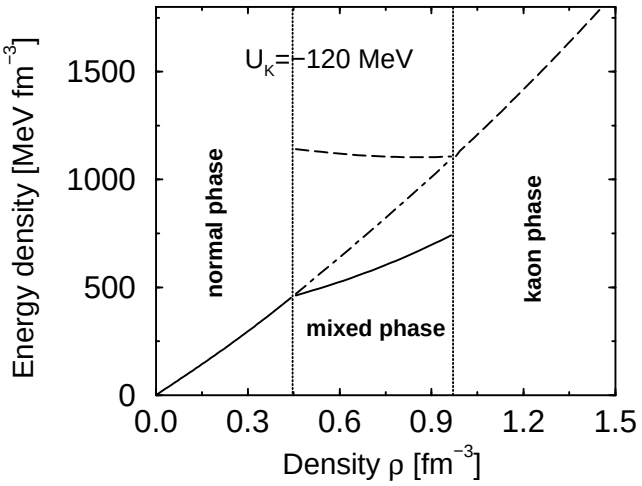

Figure 10: The energy density of normal phase (solid) and kaon condensed phase (dashed). The total energy is the volume weighted sum (dash-dotted).

in a star depending on which method is used. Fig. 11 shows the distribution in the two cases. For the Maxwell construction the energy density is discontinuous at the particular radius at which the pressure has the constant value of the Maxwell construction. The discontinuity is analogous to the separation of the phases in a gravitational field that is characteristic of a substance having a single component (like the steam above water in H_2O). As we discussed earlier, neutron star matter in beta equilibrium does not behave like that: it has two independent components and all properties are continuous from one phase to another. The distribution of mass-energy for such a star is the continuous curve with a discontinuity in *slope* but not *value*, at the boundary between mixed phase. The central core of mixed phase is surrounded by normal dense nuclear matter. For the particular value of $U(\rho_0) = -120$ MeV, the mixed phase extends to the center of the star and the pure condensed phase does not appear.

Depending on the kaon potential $U_K(\rho_0)$, the pure kaon condensed phase may not appear in the star, even for the star at the mass limit. Such is the case in the above illustration. However, for a potential $U_K(\rho_0) = -140$ MeV, the pure kaon condensed phase would form the core of stars with a mass above about $1.1M_\odot$, and for the limiting mass star, the condensed phase would extend to about 4.5 km.

The distribution of particles in the limiting mass star is dominated by the neutron in the normal phase outside 3 km as can be seen from Fig. 12. The K^- and proton are the dominant species in the mixed phase core. Lepton populations fall rapidly, as expected, as the K^- becomes dominant. However, overall, the proton population is far less than the neutron, and there appears little justification in referring to a star

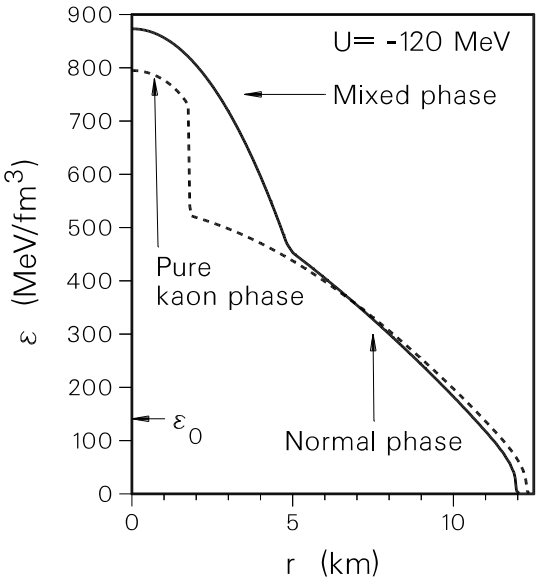

Figure 11: Mass-energy distribution according to whether the mixed phase is treated by the Maxwell construction (dashed line), or so as to respect the continuity of both chemical potentials (solid line).

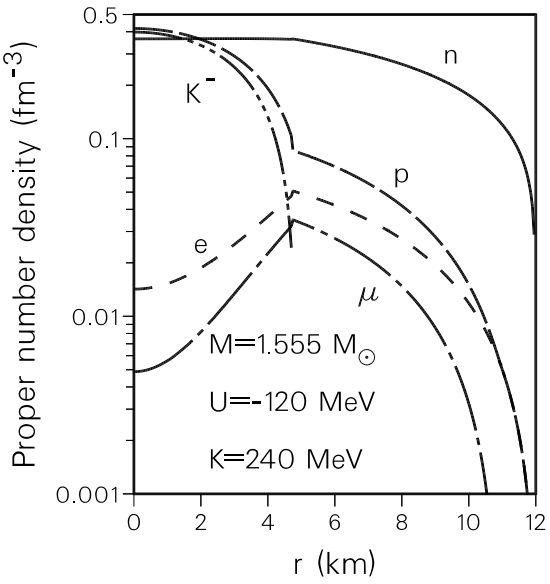

Figure 12: The composition of the maximum mass neutron star with a mass of $M = 1.555$ $M_\odot$. Note that while protons are the dominant species at the center of the star, overall, they are a minority population.

with a kaon condensate as a nucleon star.

Stellar sequences for several choices of the kaon potential $U_K(\rho_0)$ are shown in Fig. 13. Naturally the limiting mass decreases with increasing potential (for which the condensate density threshold is lower). Potentials with values only a little below $U_K(\rho_0) = -120$ MeV would not be compatible with the mass of the Hulse-Taylor pulsar, for the underlying theory of matter used here. There is a mechanical instability for the Maxwell case that is initiated by the central densities for which the pressure remains constant. In this case the *necessary* condition for stability, $dM/d\epsilon_c > 0$ is not satisfied. (The section of the dashed curve in Fig. 14 for which R is an increasing function of M is the corresponding unstable region.) Such an unstable region is absent when the phase transition is treated using Gibbs' conditions.

The mass-radius relation for several sequences is shown in Fig. 14. Comparison is made with the case corresponding to the Maxwell construction for the phase transition. It is clear that the radius especially and the limiting mass are sharp functions of $U_K(\rho_0)$. For the preferred value of $U_K(\rho_0) = -120$ MeV, radii are similar to neutron stars without the condensate. There appears to be a sharp break in behavior of M vs. R for $U_K(\rho_0) < -120$ MeV. However the behavior is actually continuous but depends sensitively on $U_K(\rho_0)$: a pure quark core develops with decreasing values of the optical potential below ~ -120 MeV and this causes the change of the radius

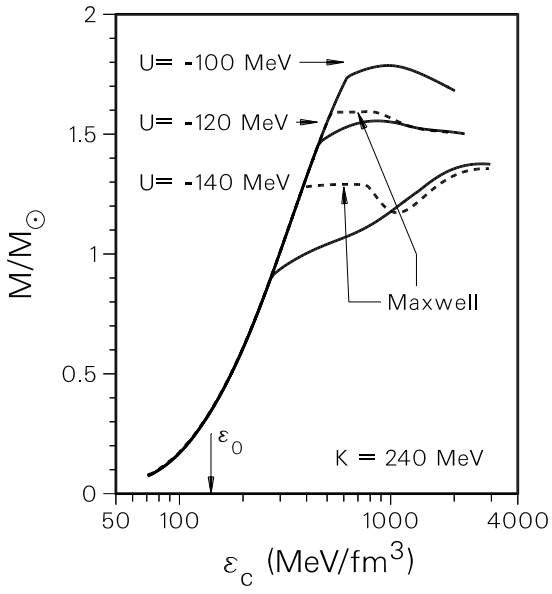

Figure 13: The mass sequence for kaon condensed neutron stars treated by the Maxwell construction (dashed line), or so as to respect the continuity of both chemical potentials (solid line).

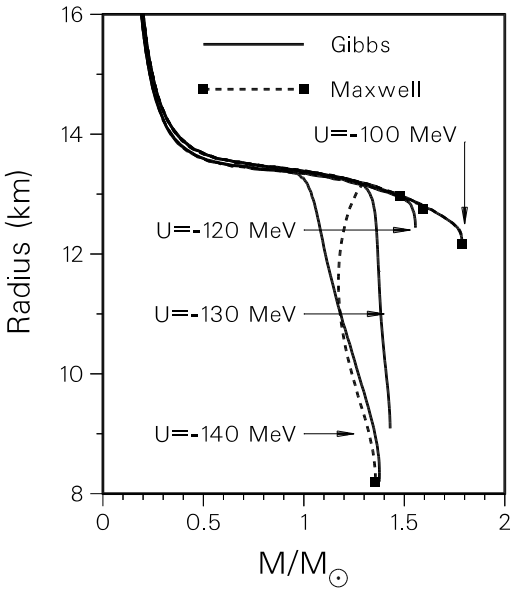

Figure 14: The mass-radius relation for kaon condensed neutron stars using a Maxwell construction (dashed line) or Gibbs condition (solid line).

from $R \approx 12.5$ km to $R \approx 8$ km for $U_K(\rho_0) = -140$ MeV.

4.2 Geometrical Structure in the Mixed Phase

Neutron star matter in the normal phase is necessarily highly isospin asymmetric since charge neutrality is imposed by the weakness of the gravitational field compared to the Coulomb force. However, since kaons are bosons, they can all occupy the zero momentum state. Consequently, when the two phases, normal and kaon condensed are in phase equilibrium, the normal phase can come closer to isospin symmetry as can be seen in Fig. 7. This is achieved by charge exchange as driven by the isospin restoring force arrising in part from the Fermi energies and in part from the coupling of the ρ meson to the nucleon isospin. Naturally, the possibility of achieving symmetry varies as the proportion of the kaon phase. Regions of normal matter will be positively charged while regions of the kaon condensed phase will be negatively charged. Charge neutrality is globally achieved in this way, but not locally. As was discussed in Ref. [2], regions of like charge will tend to be broken up into small regions while the surface interface energy will resist. The competition is resolved by formation of a Coulomb lattice much as nuclei embeded in an electron gas. The difference here is that it is two phases of nuclear matter that are involved. The rarer phase will occupy lattice sites embedded in the dominant phase. As the proportion of phases changes, the total

energy consisting of volume, surface and Coulomb energies will be minimized by a sequence of geometrical forms at the lattice sites, which we idealize as drops, rods and slabs, just as for nuclear matter embedded in a background of free electrons and neutrons [36].

Relevant details of the structure calculation can be found in Ref. [10, 11]. In the present situation, the physical quantities that determine the geometrical structure are shown in Figs. 15 and 16. Of course a calculation of the geometric structure,

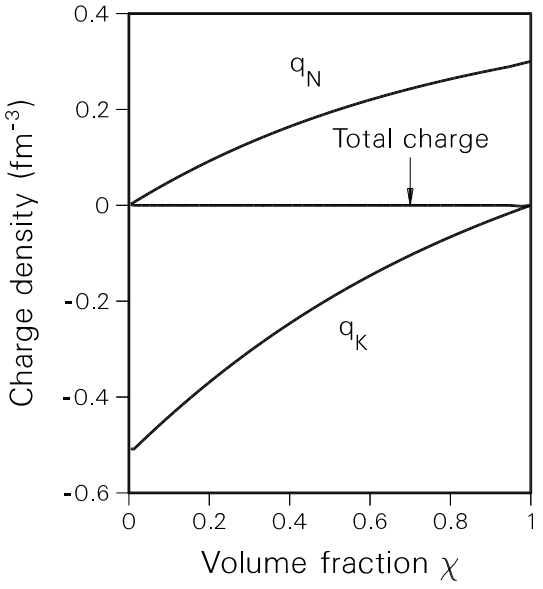

Figure 15: Charge densities in the normal and kaon condensed phase as a function of the volume fraction of the latter.

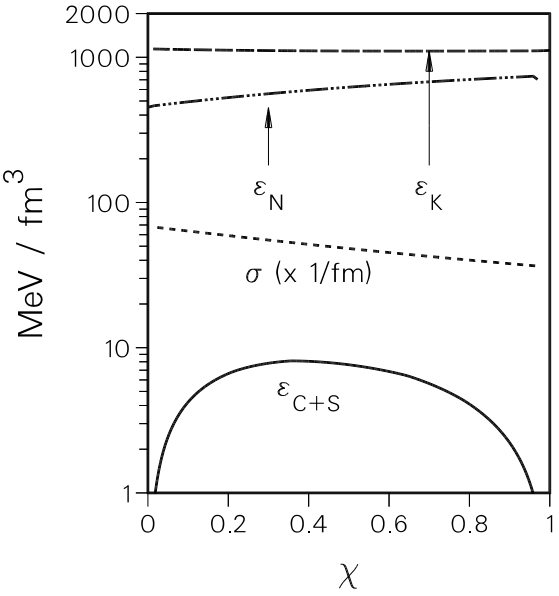

Figure 16: Bulk energy densities of normal and kaon phases as a function of the volume fraction of the kaon phase, the surface tension σ which is assumed to be proportional to their difference, and the sum of Coulomb and surface energy density.

which results from a competition between Coulomb and surface energies, requires a knowledge of the surface tension σ at the interface between the phases. This is not known although a calculation is in progress [37]. What we do know is that: (1) The sizes, spacings and the sum of Coulomb and surface energies scale as $\sigma^{1/3}$. (2) To first approximation, the locations of the transition from one geometric phase to another does not depend on σ. The reason for this is that the sum of Coulomb and surface energy densities is small compared to the bulk energy density (cf. Fig. 16). (3) The threshold density of the mixed phase and the density at which it ends is not disturbed by our uncertainty in σ because the sum of Coulomb and surface energies vanishes at the end points (Fig. 16, see eq. (2) in Ref. [10]). (4) The structured phase lies lower in energy than the unstructured (See near end of introduction of Ref. [12].) For the

above reasons the dimensions shown in Fig. 18 provide a guide but the locations of phases should be quite accurate.

The charge densities carried by the two phases and the volume fraction of the kaon phase is shown in Fig. 17 as a function of radial coordinate in the star. Outside of 5 km, matter is in the pure nuclear phase and it is chargeless, the proton population being balanced by electrons. In the idealized geometry of shapes, the kaon phase will first form at the threshold density of condensation as spheres spaced far apart. As the fraction of kaon phase increases, the spacing will decrease and eventually the spheres will merge to form rods and then slabs. As the volume fraction of the kaon phase comes to dominate, slabs of normal phase will be present in a background of kaon phase, and the role of the two phases is interchanged. The diameter and spacing of the geometrical forms of the crystal lattice is shown in Fig. 18 for the limiting mass star. The location of the boundaries of the various phases can be seen in Fig. 19 for stars of various mass.

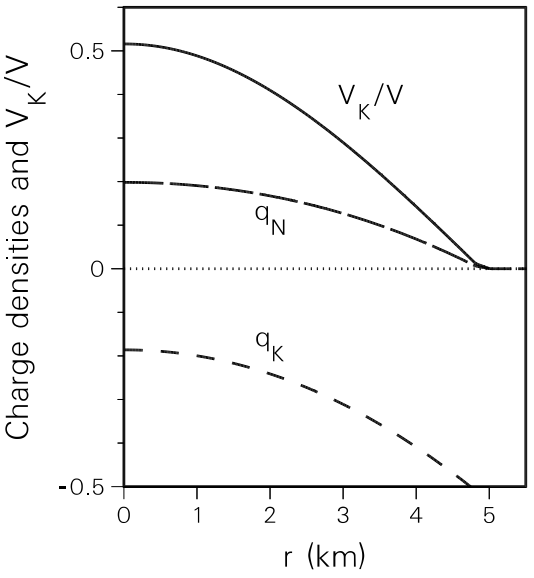

Figure 17: Charge densities in the normal and kaon condensed fractions of the mixed phase in the limiting mass star of the case $U(\rho_0) = -120$ MeV. Volume fraction of kaon phase is also plotted.

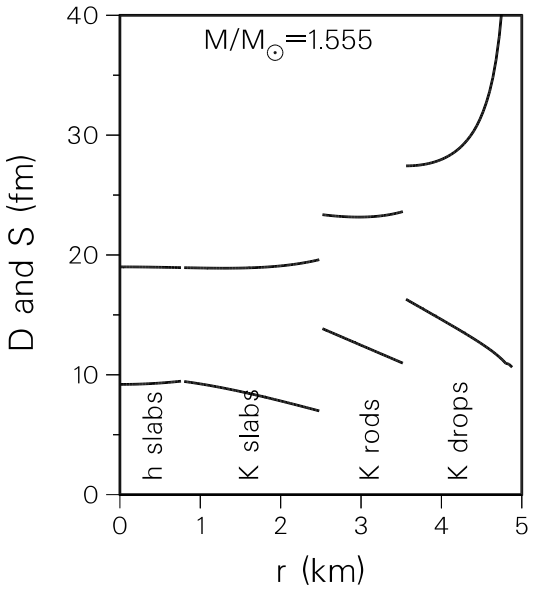

Figure 18: Diameter D of objects (drops, rods, slabs) of the rarer phase immersed in the dominant phase, located at lattice sites spaced S apart.

These are rather remarkable properties of the mixed phase, which in the model star, occupies the inner 5 km. It is filled with geometrical forms of varying shapes and spacings, according to depth in the star. The charge density within the geometrical objects and the background phase is opposite in sign and varying in magnitude with depth. Finally the effective mass of the nucleons is radically different in the two phases as can be seen in Fig. 20. All of these features must have their effect on transport

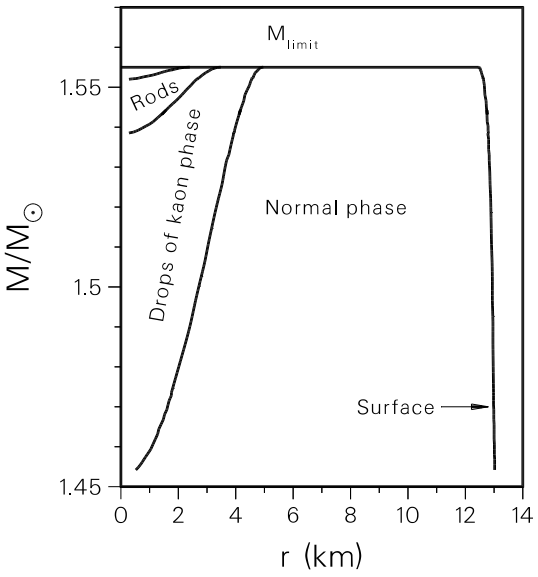

Figure 19: Radial boundaries between phases are shown for a range of stellar masses.

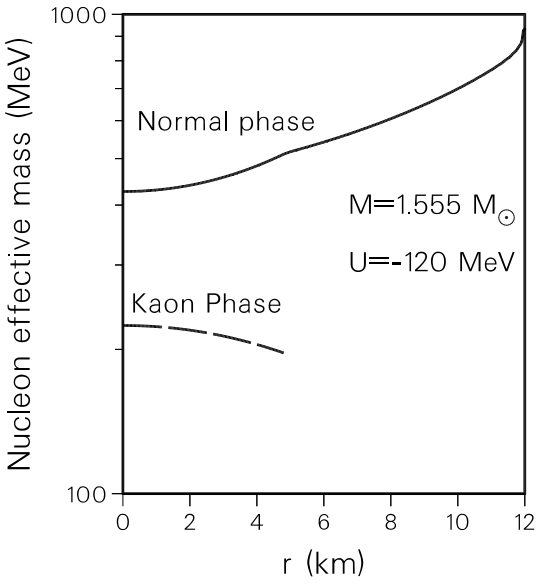

Figure 20: Nucleon effective mass in the normal and kaon condensed phase as a function of radial location in the limiting mass star.

properties and possibly on Glitch phenomena. Glitches are thought to correspond to changes induced in the moment of inertia of the star as a massive number of superfluid vortex lines undergo shifts in the location of the sites in the solid regions to which they are pinned [38]. The relocation occurs unpredictably as the instantaneous location of the vortices carrying the angular momentum come out of equilibrium with decreasing spin of the star and create stresses that are relieved by the massive unpinnings. The thin crust is a location at which the vortex lines can be pinned. But in the present model, the vortex lines do not thread through the entire star, pinned at each end on the crust, but are pinned at one end on the interior crystalline mixed phase. The extent of this region varies sensitively as the mass of the star, perhaps accounting for the wide variety in glitch phenomena observed in different pulsars.

5 Summary

We have discussed the properties of kaon condensation in neutron star matter when it is of first order. As is general for any phase transition in a substance having more than a single conserved charge, the mixed phase does occupy a finite extent in the star, and in that region is quite rich in phenomena. First, a Coulomb lattice of rare phase immersed in the dominant one will will form, having various geometries at the lattice sites, according to the pressure. This feature is common to nuclear systems having a mixed phase (independent of the phase transition) so long as the temperature is

low on the nuclear scale. Second, nucleons have different mass depending on whether they are in the objects at the lattice sites, or in the background medium. Third, the objects at the lattice sites have opposite charge compared to the background. Thus the mixed phase region, which we calculate to occupy a region of a few kilometers in extent, is highly heterogeneous. We believe this will be an important factor in determining the transport properties of this region. Moreover, the solid region, if present, is likely to play a role in the pulsar glitch phenomenon and its extent in the core, being very sensitive to stellar mass, may account for the variety of glitch phenomena observed in different pulsars.

Acknowledgments

J. S.-B. acknowledges support by the Alexander von Humboldt-Stiftung. This work was supported by the Director, Office of Energy Research, Office of High Energy and Nuclear Physics, Division of Nuclear Physics, of the U.S. Department of Energy under Contract DE-AC03-76SF00098.

References

[1] N. K. Glendenning, Nucl. Phys. B (Proc. Suppl.) **24B** (1991) 110.

[2] N. K. Glendenning, Phys. Rev. D **46** (1992) 1274.

[3] J. B. Hartle, R. F. Sawyer and D. J. Scalapino, Astrophys. J. **199** (1975) 471.

[4] W. Weise and G. E. Brown, Phys. Lett. **58B** (1975) 300.

[5] A. B. Migdal, A. I. Chernoustan and I. N. Mishustin, Phys. Lett. **83B** (1979) 158.

[6] A. B. Migdal, in *Mesons in Nuclei, Vol III* edited by M. Rho and D. Wilkinson (North-Holland Publishing Co., 1979) p. 941, see esp. p. 978.

[7] S.-O. Backman and W. Weise in *Mesons in Nuclei, Vol III* edited by M. Rho and D. Wilkinson (North-Holland Publishing Co., 1979) p. 1095, see esp. p. 1116.

[8] H. Heiselberg, C. J. Pethick, and E. F. Staubo, Phys. Rev. Lett. **70** (1993) 1355.

[9] V. R. Pandharipande and E. F. Staubo, in *Proc. 2'nd International Conf. of Physics and Astrophysics of Quark-Gluon Plasma,* Calcutta, 1993, Eds. B. Sinha, Y. P. Viyogi and S. Raha, (World Scientific, 1994).

[10] N. K. Glendenning and S. Pei, Phys. Rev. C **52** (1995) 2250.

[11] N. K. Glendenning and S. Pei, (in the Eugene Wigner Memorial Issue of) Heavy Ion Physics (Budapest)**1** (1995) 1.

[12] M. B. Christiansen and N. K. Glendenning, Phys. Rev. C **56** (1997) 2858.

[13] U. Heinz, K. S. Lee, and M. Rhoades-Brown, Mod. Phys. Lett. A **2** (1987) 153.

[14] C. Greiner, P. Koch, and H. Stöcker, Phys. Rev. Lett. **58**, 1825 (1987).

[15] N. K. Glendenning, Astrophys. J. **293** (1985) 470.

[16] D. B. Kaplan and A. E. Nelson, Phys. Lett. B **175**, 57 (1986), ibid B 179, 409 (E).

[17] G. E. Brown, K. Kubodera, M. Rho, and V. Thorsson, Phys. Lett. B **291**, 355 (1992).

[18] V. Thorsson, M. Prakash, and J. M. Lattimer, Nucl. Phys. A **572**, 693 (1994).

[19] H. Fujii, T. Maruyama, T. Muto, and T. Tatsumi, Nucl. Phys. A **597**, 645 (1996).

[20] G. Q. Li, C.-H. Lee, and G. E. Brown, Phys. Rev. Lett. **79**, 5214 (1997).

[21] N. K. Glendenning and J. Schaffner-Bielich, Phys. Rev. Lett. (to be published).

[22] A. Faessler, A. J. Buchmann, and M. I. Krivoruchenko, Phys. Lett. B **391**, 255 (1997).

[23] N. K. Glendenning and J. Schaffner-Bielich, Phys. Rev. C **58**, 1298 (1998).

[24] J. Boguta and A. R. Bodmer, Nucl. Phys. A **292**, 413 (1977).

[25] N. K. Glendenning, *COMPACT STARS, Nuclear Physics, Particle Physics, and General Relativity* (Springer–Verlag New York, 1997).

[26] N. K. Glendenning and S. A. Moszkowski, Phys. Rev. Lett. **67**, 2414 (1991).

[27] T. Waas, N. Kaiser, and W. Weise, Phys. Lett. B **379**, 34 (1996).

[28] V. Koch, Phys. Lett. B **337**, 7 (1994).

[29] T. Waas and W. Weise, Nucl. Phys. A **625**, 287 (1997).

[30] E. Friedmann, A. Gal, and C. J. Batty, Nucl. Phys. A **579**, 518 (1994).

[31] W. H. Dickhoff, A. Faessler, H. Müther, and S. S. Wu, Nucl. Phys. A **405**, 534 (1983).

[32] M. Lutz, Phys. Lett. B **426**, 12 (1998).

[33] J. Schaffner-Bielich, I. N. Mishustin, and J. Bondorf, Nucl. Phys. A **625**, 325 (1997).

[34] G. E. Brown, C.-H. Lee, M. Rho, and V. Thorsson, Nucl. Phys. A **567**, 937 (1994).

[35] We thank Hirotsugu Fujii for providing us with the data tables to check the neutron population from [19].

[36] D. G. Ravenhall, C. J. Pethick and J. R. Wilson, Phys. Rev. Lett. **50** (1983) 2066.

[37] M. Christiansen, private communication, Oct., 1998.

[38] M. A. Alpar, H. F. Chau, K. S. Cheng, and D. Pines, Astrophys. J. **459**, 706 (1996).